

# High-speed silicon-organic hybrid modulator enabled by sub-wavelength grating waveguide ring resonator

Zeyu Pan<sup>1</sup>, Xiaochuan Xu<sup>2</sup>, Chi-Jui Chung<sup>1</sup>, Hamed Dalir<sup>2</sup>, Hai Yan<sup>1</sup>, Ke Chen<sup>3</sup>, Yaguo Wang<sup>3</sup>, Baohua Jia<sup>4</sup>, and Ray T. Chen<sup>1,2</sup>

<sup>1</sup>Department of Electrical and Computer Engineering, The University of Texas at Austin, 10100 Burnet Rd, MER 160, Austin, TX 78758, USA

<sup>2</sup>Omega Optics, Inc., 8500 Shoal Creek Blvd, Austin, TX 78757, USA

<sup>3</sup>Department of Mechanical Engineering, The University of Texas at Austin, Austin, TX 78712, USA

<sup>4</sup>Centre for Micro-Photonics, Swinburne University of Technology, John Street, Hawthorn, Victoria 3122, Australia

Author e-mail address: xiaochuan.xu@omegaoptics.com, chenrt@austin.utexas.edu

**Abstract:** We present a high-speed modulator based on electro-optic polymer infiltrated sub-wavelength grating waveguide ring resonator. A 3-dB small signal modulation bandwidth of 41.36 GHz has been demonstrated. © 2018 The Author(s)

**OCIS codes:** (050.6624) Subwavelength structures; (130.4110) Modulators

Silicon photonics [1] has been widely accepted as one of the essential technologies in the next generation optical interconnect [2]. One of the intrinsic obstacles is the absence of  $\chi^{(2)}$ -nonlinearity in unstrained silicon due to its centrosymmetric crystal structure, making modulating photons on silicon platform a great challenge. The silicon-organic hybrid (SOH) platform enables the marriage of the best of the two worlds and thus has been receiving substantial attention. Compared to plasma dispersion, electro-optic (EO) polymers have a remarkable EO coefficient ( $r_{33} > 400 \text{ pm/V}$ ), ultrafast response speed ( $< 1 \text{ fs}$ ), small dispersion, and spin-casting compatibility, which promise low-power consumption, ultra-high speed operation, and ease of fabrication [2].

In this paper, we report a subwavelength grating (SWG) ring resonator based modulator. Compared to slot waveguide, SWG provides competitive mode volume overlap and a comparable propagation loss as strip waveguides. A 3-dB small signal modulation bandwidth of 41.36 GHz has been observed. The ring occupies only an area of  $70 \mu\text{m} \times 29 \mu\text{m}$ . According to the authors' best knowledge, it is the most compact and fastest ring resonator modulator that has been demonstrated on the SOH platform.

The schematic of SWG waveguides [7] is shown in Fig. 1(a). The hybrid waveguide core is formed by periodically interlacing segments of high and low refractive index materials at a subwavelength pitch. The top and bottom claddings are EO polymer SEO125 (Soluxra LLC) and silicon dioxide, respectively. The optical mode propagates along the  $z$ -direction and its optical properties can be tuned by adjusting the period ( $P$ ), waveguide width ( $W$ ), pillar length ( $L$ ), and Si thickness ( $H$ ). The simulated photonic band structure of the SEO125/silicon SWG waveguides, using the 3D plane wave expansion method (RSoft, inc.), is shown in Fig. 1(b). The black line represents the light line of SEO125 ( $n=1.63$ ). The solid and dashed lines denote even- and odd-like modes, respectively, which are categorized according to their parities with respect to the central slab plane in the  $y$ -direction. When the modes are away from the edge of reduced Brillouin zone, the dispersion characteristic of the guided modes resembles that of a uniform waveguide. The electrical fields  $|E_x|^2$  of optical modes at  $x$ -slice ( $x = 0 \mu\text{m}$ ),  $y$ -slice ( $y = 0 \mu\text{m}$ ), and  $z$ -slice ( $z = 0 \mu\text{m}$ ) are plotted in Fig. 1(c), (d), and (e), respectively. It can be observed that there is a strong optical field exists outside Si pillars in the SEO125 region. The mode volume overlap integral  $f = \int_{\text{SEO125}} \epsilon E^2 dv / \int_{\text{total}} \epsilon E^2 dv$  is adopted to quantify the optical field in SEO125. In this paper, SWG is optimized to operate at  $\lambda_0 = 1565 \text{ nm}$ , and we will focus on the fundamental TE-like mode (blue solid line in Fig. 1(b)). To ensure the SWG structure operates in the subwavelength regime and ease of fabrication, we choose the period  $P = 250 \text{ nm}$ , and the pillar length  $L = 175 \text{ nm}$ , corresponding to a filling factor of 0.7, along with the waveguide width  $W = 500 \text{ nm}$ . In this configuration, The overlap integral is 36.2%. Compared to the overlap integral of typical strip waveguide ( $\sim 4.0\%$ ), it increases around nine times.

The proposed SWG ring resonator based modulator is shown in Fig. 1(f). Subwavelength grating couplers are exploited to interfacing single mode fibers. Rounded rectangular shape is adopted instead of the most common circular shape to gain more flexibility in tuning the coupling strength between the bus waveguide and the ring resonator. As shown in Fig. 1(f), the shape of the ring resonator is defined by the coupling length  $L_c$ , phase shifter length  $L_a$ , and bending radius  $R$ , which are  $9 \mu\text{m}$ ,  $50 \mu\text{m}$ , and  $10 \mu\text{m}$ , respectively. Due to the compact size, the walk-off between electrical and optical signal is negligible. Thus, high speed modulation can be readily achieved with lumped electrodes. It has been proved that without 50 Ohm termination, lumped electrodes can effectively reduce the power consumption compared to traveling wave electrodes. The zoomed-in schematic of the SWG ring resonator is shown in Fig. 1(g). The central width, gold thickness, and gap are  $25 \mu\text{m}$ ,  $2.4 \mu\text{m}$ , and  $4 \mu\text{m}$  respectively. The SEM of the fabricated SWG ring resonator is shown in Fig. 1(h-l).

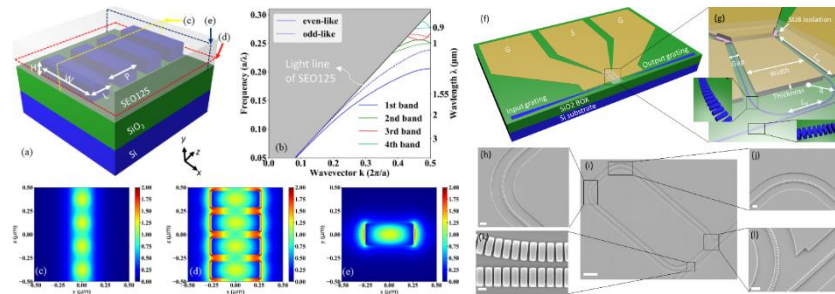


Fig. 1. (a) Schematic of a SWG waveguide for the optical modulator. (b) Photonic band structure of for SWG waveguides with SEO125 as top cladding for the waveguide width  $W = 500 \text{ nm}$  and pillar length  $L = 150 \text{ nm}$ . The y-axis on the right side is wavelength  $\lambda$  corresponding to the period  $P = 250 \text{ nm}$ . The electrical field distribution of the SWG waveguide at (c)  $x$ -slice ( $x = 0 \mu\text{m}$ ), (d)  $y$ -slice ( $y = 0 \mu\text{m}$ ), and (e)  $z$ -slice ( $z = 0 \mu\text{m}$ ). (f) Schematic of an EO polymer modulator based on the SWG ring resonator. (g) The zoomed-in schematic of the SWG ring resonator. SEM images of the fabricated SWG ring resonator (i) and zoomed in images (h) (j) (k) and (l). The white bar in (h-l) indicates  $1 \mu\text{m}$ ,  $10 \mu\text{m}$ ,  $1 \mu\text{m}$ ,  $0.2 \mu\text{m}$ , and  $1 \mu\text{m}$ , respectively.

The transmission of the fabricated SWG ring resonator is characterized by amplified spontaneous emission (ASE) broad band source and optical spectrum analyzer. To optimize the gap between bus waveguide and the ring, a set of devices with different gaps are fabricated and measured. The spectra are summarized in Fig. 2(a). The maximum extinction ratio is 27.89 dB, corresponding to an edge-to-edge gap of 500 nm between the bus waveguide and the ring resonator. The EO-polymer is poled at  $150^\circ\text{C}$  for 1 minute to align the chromophore molecules. To characterize the poling efficiency, DC voltage is applied on the electrodes with a configuration shown as the inset of Fig. 2(b). The red shift of the resonance is observed and plotted in Fig. 2(b). The averaged resonance shift of 41.28 pm/V. Thus, from the electro-optic effect  $\Delta n = \frac{1}{2} r_{33} n^3 \frac{V}{d}$ , the EO coefficient is estimated to  $r_{33} = 54.72 \text{ pm/V}$ . Then, the estimated poling efficiency is 43.78% to the EO coefficient of the bulk EO polymer. The measured and normalized response of the SWG optical modulator is shown in Fig. 2(c). The 3-dB bandwidth is 41.36 GHz, and the 6-dB bandwidth is 44.08 GHz. The measured optical transmission spectra of the modulator operating at 8-26 GHz, as shown in Fig. 2(d). The modulation index versus frequency is shown in Fig. 2(e). The modulation index results are normalized to a 10 dBm launch power. Since lumped electrodes are exploited, the power consumption is equivalent to charging and discharging two capacitors. The total capacitance is estimated to be 0.40 fF. According to Fig. 2(b), assuming  $V_{pp}=5\text{V}$  is selected, which corresponds to a 6 dB on-off ratio, the power consumption can be estimated as:  $\frac{1}{4} CV^2 = 2.55 \text{ fJ/bit}$ .

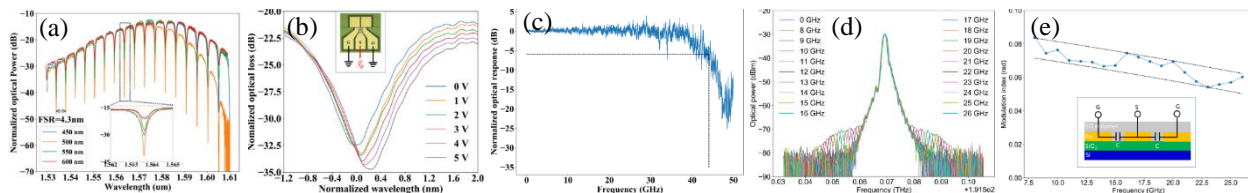


Fig. 2. (a) The normalized optical spectra with the gap size 450 nm, 500 nm, 550 nm and 600 nm. (b) The spectrum resonance shift after applied the electric field. The DC voltage is applied on the electrodes with a configuration in the insert of (b). (c) The measured and normalized optical response versus the frequency. (d) The measured optical transmission spectra of the modulator operating at 8-26 GHz. (e) The modulation index versus frequency. The modulation index results are normalized to a 10 dBm launched power.

We have demonstrated the first high speed optical modulator based on electro-optic polymer infiltrated subwavelength grating waveguide ring resonator. SWG structure increases the interactive volume between optical signal and EO polymer by 9 times. The measured 3-dB bandwidth is 41.36 GHz. The power consumption for digital communication is 2.55 fJ/bit. The bandwidth can be further increased and the power consumption can be further decreased by increasing the filling factor.

This research is supported by the US Department of Energy Contract #: DE-SC0013178.

## References

1. R. Soref, "The Past, Present, and Future of Silicon Photonics," *IEEE J. Sel. Top. Quantum Electron.* **12**, 1678–1687 (2006).
2. H. Subbaraman, Z. Pan, C. Zhang, Q. Li, L. J. Guo, and R. T. Chen, "Printed polymer photonic devices for optical interconnect systems," in *Photonics West* (SPIE, 2016), Vol. 9753, p. 97530Y–97530Y–10.
3. R. Ding, Y. Liu, Q. Li, Y. Yang, Y. Ma, K. Padmaraju, A. E.-J. Lim, G.-Q. Lo, K. Bergman, T. Baehr-Jones, and M. Hochberg, "Design and characterization of a 30-GHz bandwidth low-power silicon traveling-wave modulator," *Opt. Commun.* **321**, 124–133 (2014).
4. G. P. Agrawal, *Lightwave Technology: Components and Devices* (John Wiley & Sons, 2004).
5. D. J. Thomson, F. Y. Gardes, J. M. Fedeli, S. Zlatanovic, Y. Hu, B. P. P. Kuo, E. Myslivets, N. Alic, S. Radic, G. Z. Mashanovich, and G. T. Reed, "50-Gb/s silicon optical modulator," *IEEE Photonics Technol. Lett.* **24**, 234–236 (2012).
6. L. Alloati, R. Palmer, S. Diebold, K. P. Pahl, B. Chen, R. Dinu, M. Fournier, J.-M. Fedeli, T. Zwick, W. Freude, C. Koos, and J. Leuthold, "100 GHz silicon-organic hybrid modulator," *Light Sci. Appl.* **3**, e173 (2014).
7. H. Yan, X. Xu, C.-J. Chung, H. Subbaraman, Z. Pan, S. Chakravarty, and R. T. Chen, "One-dimensional photonic crystal slot waveguide for silicon-organic hybrid electro-optic modulators," *Opt. Lett.* **41**, 5466 (2016).